Estuarine, Coastal and Shelf Science 178 (2016) 158–167

Contents lists available at ScienceDirect

Estuarine, Coastal and Shelf Science

journal homepage: www.elsevier.com/locate/ecss

Absorption properties of high-latitude Norwegian coastal water: The impact of CDOM and particulate matter

Ciren Nima [a, b, *], Øyvind Frette [a], Børge Hamre [a], Svein Rune Erga [c], Yi-Chun Chen [a], Lu Zhao [a], Kai Sørensen [d], Marit Norli [d], Knut Stamnes [e], Jakob J. Stamnes [a]

[a] Department of Physics and Technology, University of Bergen, Norway
[b] Department of Physics, Tibet University, China
[c] Department of Biology, University of Bergen, Norway
[d] Norwegian Institute for Water Research, Norway
[e] Stevens Institute of Technology, USA

ARTICLE INFO

Article history:
Received 22 October 2015
Received in revised form
9 April 2016
Accepted 12 May 2016
Available online 18 May 2016

Keywords:
High-latitude coastal water
Colored dissolved organic matter
Total suspended matter
Phytoplankton
Chlorophyll-*a* specific absorption coefficient of phytoplankton
Non-algal particles

ABSTRACT

We present data from measurements and analyses of the spectral absorption due to colored dissolved organic matter (CDOM), total suspended matter (TSM), phytoplankton, and non-algal particles (NAP) in high-latitude northern Norwegian coastal water based on samples taken in spring, summer, and autumn. The Chlorophyll-*a* (Chl-*a*) concentration was found to vary significantly with season, whereas regardless of season CDOM was found to be the dominant absorber for wavelengths shorter than 600 nm. The absorption spectral slope $S_{350-500}$ for CDOM varied between 0.011 and 0.022 nm^{-1} with mean value and standard deviation given by (0.015 ± 0.002) nm^{-1}. The absorption spectral slope was found to be strongly dependent on the wavelength interval used for fitting. On average, $S_{280-500}$ was found to be 43% higher than $S_{350-500}$. A linear relationship was found between the base 10 logarithm of the absorption coefficient at 440 nm [$\log(a_g(440))$] and $S_{350-500}$. Regardless of season, phytoplankton were the dominant component of the TSM absorption indicating little influence from land drainage. The mean values of the Chl-*a* specific absorption coefficient of phytoplankton $a^*_{ph}(\lambda)$ at 440 nm and 676 nm were 0.052 m^2 mg^{-1} and 0.023 m^2 mg^{-1}, respectively, and $a^*_{ph}(\lambda)$ was found to vary with season, being higher in summer and autumn than in spring. The absorption spectral slope S_{NAP}, which is the spectral slope of absorption spectrum for non-algal particles, was lower than that for European coastal water in general. It varied between 0.0048 and 0.022 nm^{-1} with mean value and standard deviation given by $(0.0083^{-1} \pm 0.003)$ nm^{-1}. Comparisons of absorption coefficients measured *in situ* using an ac-9 instrument with those measured in the laboratory from water samples show a good agreement.

1. Introduction

Coastal water bodies are generally classified as Case 2 water, in which non-algal particles and colored dissolved organic matter (CDOM) contribute significantly to the optical properties in addition to phytoplankton. These three constituents vary independently in Case 2 water and tend to be highly variable in space and time. In contrast, the optical properties in open oceanic (Case 1) water are relatively stable over large spatial and temporal scales due to limited terrestrial and anthropogenic impacts. Several studies have revealed variation in the optical properties from high-latitude to low- and mid-latitude water (Mitchell and Holm-Hansen, 1991; Dierssen and Smith, 2000; Sathyendranath et al., 2001). Currently used remote-sensing algorithms for estimating pigment concentrations from ocean color data, such as OC2V4 and OC4V4, are based mainly on *in situ* data collected in low- and mid-latitude water bodies, restricting their use for estimation of Chlorophyll-*a* (Chl-*a*) concentrations in high-latitude water (Stramska et al., 2003). For northern high-latitude water (Sathyendranath et al., 2001; Stramska et al., 2003, 2006) few *in situ* data are available for construction of reliable algorithms for ocean color remote sensing. Therefore, extensive measurements and analyses of optical properties for northern high-latitude water are needed in order to provide knowledge of optical properties and improve

* Corresponding author. Department of Physics and Technology, University of Bergen, Norway.
E-mail address: tseringtu@yahoo.com (C. Nima).

http://dx.doi.org/10.1016/j.ecss.2016.05.012

ocean color based estimation. In addition, application of regional bio-optical models combined with radiative transfer models valid for coupled atmosphere-ocean systems can significantly improve the retrieval accuracy for marine parameters in Case 2 water.

Knowledge of inherent optical properties (IOPs) and concentrations of optically significant water constituents is essential for determining the underwater light climate, water clarity, and heat budget. The absorption properties of water constituents, such as CDOM and particulate matter, strongly influence the penetration of light in coastal water, and hence determine the availability of photosynthetically active radiation (PAR) that can be utilized by photosynthetic algae for primary production. The spectral absorption coefficient is an important parameter that can be used to derive semi-analytical relationships with the remote-sensing reflectance.

CDOM absorption has been studied both for Case 1 and Case 2 water (Bricaud et al., 1981; Stedmon et al., 2000; Højerslev and Aas, 2001; Babin et al., 2003; Twardowski et al., 2004; Nelson and Siegel, 2013; Hancke et al., 2014; Matsuoka et al., 2015), and the absorption spectral slope S is an important parameter used to characterize it. S can be a useful indicator of changes in the composition of CDOM due to mixing of waters of different origins (Conmy et al., 2004) or photo-bleaching (Helms et al., 2008). Also, S is related to the average molecular weight of CDOM (Helms et al., 2008) and bacterial production and abundance (Matsuoka et al., 2015). Stedmon and Markager (2001) and Matsuoka et al. (2011) found an inverse relationship between the CDOM absorption coefficient at a certain wavelength and the CDOM spectral slope, whereas Vodacek et al. (1997) and Babin et al. (2003) did not find such a relationship. Several authors have pointed out that S depends strongly on the wavelength interval used for fitting (Twardowski et al., 2004; Nelson and Siegel, 2013). But in most studies, S has been derived only for one wavelength interval, which varies between studies. Nevertheless, S values derived using different wavelength intervals have been compared in many studies, thus obscuring the real difference between S values for different water bodies.

Bricaud et al. (1998) proposed a parameterization of particulate or phytoplankton absorption as a function of the Chl-*a* concentration for Case 1 water at mid- and low-latitude regions. The empirical relation they developed can be used to predict the particulate or phytoplankton absorption for a given Chl-*a* concentration. In Case 2 water, one expects a high structural and compositional variability of phytoplankton. Also, there are differences in the optical properties between high-latitude and low- and mid-latitude water (Sathyendranath et al., 2001).

Studies of the optical properties of coastal and fjord water have been carried out extensively in the past decades (Stedmon et al., 2000; Højerslev and Aas, 2001; Babin et al., 2003; Hamre et al., 2003; Frette et al., 2004; Erga et al., 2012), partly because of strong interest due to fisheries and aquaculture activities, but also to assess impact from human activities as well as to improve satellite-based monitoring of coastal water bodies.

The present study took place in the waters around the island of Røst, the outermost island in the Lofoten archipelago. In this area, the Northeast Arctic cod stock comes in for spawning in March–April (Röhrs et al., 2014). This yearly event is the basis for the world' s largest cod fishery, making this area particularly important. Also, Vestfjorden, which is adjacent to our study site, is known for its complex oceanography. It is the meeting place for two major current systems, the Norwegian Atlantic Current (NAC) and the Norwegian Coastal Current (NCC) (Mitchelson-Jacob and Sundby, 2001). Thus, Vestfjorden is an important and challenging site to study with respect to environmental impact on the ecosystem and sustainable management of the valuable cod stock. In this study, we present: (1) measurements and analyses of the absorption properties of CDOM, phytoplankton, and non-algal particles for northern high-latitude coastal water close to the island of Røst in the Lofoten archipelago in different seasons, (2) seasonal variation of the concentrations of Chl-*a* and TSM, (3) seasonal variation of the Chl-*a* specific absorption, and (4) comparisons of the absorption measured in the field using an ac-9 instrument and that measured in the laboratory using a spectrophotometer.

2. Data and methods

Our study area is located close to the island of Røst in Northern Norway, just above the Arctic Circle, as shown in Fig. 1. Røst is the outermost island in the Lofoten archipelago, and this area is adjacent to Vestfjorden and the Norwegian Sea. Vestfjorden is an open coastal fjord between the Lofoten islands and the mainland of Norway. The upper layers of the Norwegian Sea are dominated by warm, salty Atlantic water, whereas Norwegian coastal areas are influenced by water of lower salinity and seasonally varying temperature that is transported northward by the NCC (Loeng and Drinkwater, 2007). The circulation patterns and hydrographic conditions in the Norwegian Sea are strongly influenced by large-scale atmospheric pressure patterns (Loeng and Drinkwater, 2007).

We carried out measurements of IOPs at a total of 22 stations (see Table 1) in the sea close to Røst on 6 cruises during 2012–2015. At most stations, water samples were collected from three depths, i.e. close to the surface, at half the Secchi depth, and at the full Secchi depth. Detailed information about the stations is given in Table 1.

During the October 2014 and March 2015 cruises, an ac-9 instrument from WET Labs was used to simultaneously measure the *in situ* absorption coefficient a and the attenuation coefficient c at wavelengths of 412, 440, 488, 510, 532, 555, 650, 676, and 715 nm. The acceptance angle for beam transmission of an ac-9 instrument is 0.93° (WET-Labs, 2011). The ac-9 instrument was calibrated at the factory just before the cruise of October 2014. In addition to this factory calibration, we performed calibration of the ac-9 instrument using Milli-Q water before every cruise. Measurements were performed at the water sampling depths. Three types of corrections were applied to the ac-9 raw data in the following order: temperature-dependent absorption correction, salinity correction, and scattering correction. Temperature correction for both the absorption coefficient a and the attenuation coefficient c at 715 nm as well as salinity correction for both a and c at each of the 9 wavelengths were performed according to the ac-9 Meter Protocol document (WET-Labs, 2011). The *in situ* water temperature was not measured at the time of the ac-9 measurements during the October 2014 and March 2015 field campaigns, but was retrieved from the marine research website (http://www.imr.no/forskning/forskningsdata/stasjoner/) by averaging temperatures from the two stations closest to our study site (i.e. Eggum and Skrova) at the similar time. The temperature was estimated to be 9.5 °C in October 2014 and 4.7 °C in March 2015. Scattering correction was performed by subtracting the temperature-corrected absorption coefficient at 715 nm [$a(715)$] from the measured absorption coefficient at each of the 9 wavelengths to obtain $a(\lambda)$ (WET-Labs, 2011). After these corrections, to further control the data quality, some of the surface data that showed significant fluctuations, mainly due to air bubbles made by surface waves, were discarded.

a Determination of CDOM Absorption Coefficient and Spectral Slope

Water samples were filtered through Whatman Polycarbonate filters (diameter 47 mm, pore size 0.22 μm) at low vacuum pressure

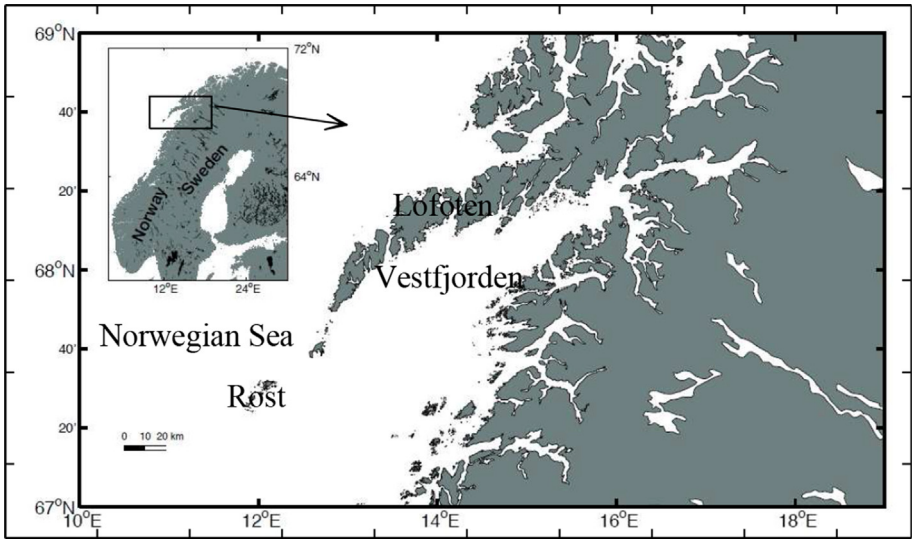

Fig. 1. Map of Lofoten archipelago, Vestfjorden, the Norwegian Sea, and Røst island in Northern Norway.

Table 1
Station (St.), Location, Secchi depth, and date for each measurement in coastal water close to the island of Røst, Northern Norway. Stations are ordered chronologically according to measurement date.

St.	Location	Secchi depth [m]	Date
1	67° 27.000′N 12° 02.800′E	12	07/30/2012
2	67° 27.100′N 12° 06.000′E	12	07/31/2012
3	67° 28.200′N 11° 56.500′E	10	08/01/2012
4	67° 26.567′N 11° 58.570′E	9	04/29/2013
5	67° 27.040′N 11° 59.870′E	10	05/01/2013
6	67° 28.813′N 12° 00.273′E	8	05/02/2013
7	67° 29.130′N 12° 07.450′E	10	05/03/2013
8	67° 28.390′N 12° 11.370′E	13	10/16/2013
9	67° 28.578′N 11° 59.787′E	16	10/16/2013
10	67° 28.121′N 11° 59.242′E	14	10/17/2013
11	67° 28.477′N 11° 59.417′E	14	04/08/2014
12	67° 28.813′N 12° 00.273′E	9	04/08/2014
13	67° 28.500′N 12° 10.900′E	13	10/13/2014
14	67° 28.500′N 12° 10.900′E	12	10/14/2014
15	67° 27.017′N 12° 00.467′E	14	10/15/2014
16	67° 27.551′N 11° 59.115′E	15	10/15/2014
17	67° 32.970′N 12° 02.145′E	15	10/16/2014
18	67° 32.880′N 12° 11.230′E	12	10/16/2014
19	67° 28.772′N 12° 00.167′E	14	03/16/2015
20	67° 28.734′N 12° 07.356′E	15	03/17/2015
21	67° 32.252′N 12° 12.840′E	15	03/18/2015
22	67° 33.155′N 12° 09.260′E	15	03/18/2015

on the day of collection, and the filtrate was placed in pre-washed bottles. The bottles were first rinsed three times with filtered sample water to minimize the possibility of contamination. At some locations and depths duplicate and triplicate samples were prepared. The CDOM samples were stored in a refrigerator until analysis. Absorbance spectra of CDOM samples collected in 2012 were measured at the Norwegian Institute for Water Research (NIVA) and recorded at wavelengths in the range from 350 to 800 nm with 10 nm increments using a Perkin Elmer Lambda 40, UV/VIS spectrometer equipped with a 10 cm quartz cuvette. The rest of the samples were measured at the University of Bergen. Prior to analysis, the CDOM samples and the Milli-Q water were acclimated to room temperature. Absorbance spectra were recorded at wavelengths in the range from 200 to 900 nm with 2 nm increments using a dual-beam Shimadzu spectrophotometer (UV-1800) equipped with a 10 cm quartz cuvette. Baseline data were obtained by filling Milli-Q water both in the sample and reference cells, and baseline correction was done by subtracting the offset from each sample spectrum. Absorbance data were converted to absorption coefficients using

$$a_{g,m}(\lambda) = 2.303 OD(\lambda)/\ell, \quad (1)$$

where the subscript g stands for 'gelbstoff', which is the German name for CDOM, and m stands for measured. Further, $a_{g,m}(\lambda)$ and $OD(\lambda)$ are the measured absorption coefficient [m^{-1}] and absorbance, respectively, at wavelength λ, and ℓ is the path length in [m] (ℓ = 0.1 m). In Eq. (1), the number 2.303 is the conversion factor between the base 10 logarithm and the natural logarithm. The absorption coefficient was corrected for scattering due to residual particles in the CDOM samples by subtracting the absorption coefficient averaged over a 5-nm interval around 685 nm from all the spectral values (Babin et al., 2003).

To determine the absorption spectral slope S for CDOM, after correction for scattering, each absorption spectrum was fitted directly to the following exponential equation (Bricaud et al., 1981)

$$a_g(\lambda) = a_g(\lambda_0)\exp[-S(\lambda - \lambda_0)], \quad (2)$$

where $a_g(\lambda)$ and $a_g(\lambda_0)$ are the absorption coefficients at an observed wavelength λ and at a reference wavelength λ_0, respectively. The absorption coefficient $a_g(\lambda_0)$ at the reference wavelength λ_0 is used to characterize the CDOM concentration in a specific type of natural water. In this study, the reference wavelength λ_0 was set to 320 or 440 nm. The spectral slope S [nm^{-1}], which is independent of the choice of λ_0, indicates how rapidly the absorption decreases with increasing wavelength. The absorption spectral slope S of CDOM was found to depend on the wavelength interval used for deriving it (Twardowski et al., 2004). Therefore, in this study the absorption coefficients within two wavelength intervals, i.e. 280–500 nm and 350–500 nm, were used to derive S by nonlinear fitting, being denoted by $S_{280-500}$ and $S_{350-500}$, respectively.

b Determination of Particle Absorption Coefficients

In order to determine absorption coefficients for particulate matter, an adequate amount of water, depending on particle load, was filtered through a 25 mm diameter glass fibre filter (Whatman, GF/F, 0.7 μm nominal pore size) at low vacuum pressure. Each

sample filter for TSM and Chl-*a* was preserved in a Petri dish, wrapped with aluminum foil, and stored in a freezer before and during transportation from Røst to Bergen. After transportation, all samples were stored at −80 °C until analysis. The absorption spectrum of the particles retained on the filter was determined according to the Transmittance-Reflectance method (Tassan and Ferrari, 2002). The transmittance and reflectance of the sample filter were measured for wavelengths between 280 and 900 nm with 2 nm increments using a dual-beam Shimadzu spectrophotometer equipped with a 60 mm integrating sphere (UV-2401 PC). The absorbance OD_s of the particles retained on the filter was converted to an equivalent absorbance OD_{sus} of the suspension using (Tassan and Ferrari, 2002)

$$OD_{sus}(\lambda) = 0.423OD_s(\lambda) + 0.479OD_s^2(\lambda). \quad (3)$$

The absorption coefficient $a_p(\lambda)$ for *all* particles was then derived from

$$a_p(\lambda) = 2.303\frac{OD_{sus}}{X}, \quad (4)$$

where X [m] is the ratio of the volume of the filtered water sample to the filter clearance area.

Bleaching of pigmented particles was performed by using a 0.1% active chlorine solution of sodium hypochlorite (NaClO) in accordance with the REVAMP protocol (Tilstone et al., 2002). The absorption coefficient $a_{ph}(\lambda)$ for pigmented particles (referred to as phytoplankton in this study) was then derived by subtracting the absorption coefficient obtained after bleaching, the non-pigmented absorption coefficient $a_{NAP}(\lambda)$, from the absorption coefficient $a_p(\lambda)$. In order to agree with the terminology used in most studies, non-pigmented particles will hereafter be called non-algal particles. The following equation was fitted to the absorption coefficients for non-algal particles:

$$a_{NAP}(\lambda) = a_{NAP}(\lambda_0)\exp[-S_{NAP}(\lambda - \lambda_0)], \quad (5)$$

where $a_{NAP}(\lambda)$ and $a_{NAP}(\lambda_0)$ are the absorption coefficients at an observed wavelength λ and at a reference wavelength λ_0, respectively. In this study, the reference wavelength λ_0 was set to 443 nm. The spectral slope S_{NAP} [nm^{-1}] was determined by fitting the measured absorption spectra for non-algal particles directly to Eq. (5) by using data between 380 and 730 nm, excluding the 400–480 and 620–710 nm ranges to avoid any absorption due to residual pigmented particles that might still be present (Babin et al., 2003).

c Determination of Total Suspended Matter (TSM) Concentration

In order to determine the TSM concentration, water samples were filtered through pre-weighed Whatman 47 mm GF/F filters to obtain TSM samples. The pre-ashed, pre-washed, and pre-weighed GF/F filters were prepared in accordance with the REVAMP protocol (Tilstone et al., 2002). After transportation, TSM samples were stored in an ultra cold freezer at −80 °C until analysis. 50 mL Milli-Q water was filtered through each TSM sample filter three times to remove any salt in accordance with the REVAMP protocol (Tilstone et al., 2002), then dried in an oven at 75 °C for 24 h, and finally cooled in a desiccator and weighed on a Mettler Toledo MT5 microbalance.

d Determination of Chl-*a* Concentration

In order to determine the Chl-*a* concentration, water samples were filtered through 25 mm or 47 mm Whatman GF/F filters on the day of collection. Sample filters were stored in Petri dishes and wrapped with aluminum foil in a freezer with dry ice before and during transportation. After transportation, all samples were stored in a freezer at −78 °C or −80 °C. In this study, both High Pressure Liquid Chromatography (HPLC) and spectrophotometry were used to determine the Chl-*a* concentrations. Spectrophotometry was used for the cruises in October 2014 and March 2015, and HPLC was used for the others. Chl-*a* concentrations were determined using HPLC as follows. The pigments were extracted from the filters for 4 h in 5 mL 90% acetone in a dark room at 20–25 °C. The samples were then sonicated for 20 s for better extraction before 1 mL was transferred to 2 mL Chromacol vials and kept in the dark at (4 ± 2) °C in the injector chamber of the HPLC (Waters 2695 Separations module). Separations of pigments were done using mobile and stationary phases according to the method of Wright (1991) and detection of Chl-*a* was done using the UV–Vis spectra measured by a Photodiode Array detector (Waters 2996) and the known retention time. Chl-*a* was quantified using the response factor from a multipoint regression of a diluted DHI (Danish Hydraulic Institute) standard with known concentration of Chl-*a*. Chl-*a* concentrations were determined spectrophotometrically as follows. The pigments were extracted from the filters in 90% acetone for 10 min in an ice-filled ultrasound bath for better extraction, and stored for 24 h in a −20 °C freezer. The pigment extracts were then filtered through a 0.45 μm syringe, and the absorbance spectra of the pigment extract were measured between 350 and 900 nm using a Perkin Elmer Lambda 40, UV/VIS spectrometer with a 1 cm quartz cuvette. The Chl-a concentration was then determined using the extinction coefficient for Chl-*a* at 664 nm in 90% acetone (87.7 L g^{-1} cm^{-1} (Jeffrey and Humphrey, 1975)).

3. Results and discussion

The complex water circulation system of the Vestfjorden area should be taken into account when analyzing the spatial and temporal variation in optical properties between spring, summer, and autumn seasons. The formation of large frontal eddies (up to 60 km in diameter) is of special interest in this context (Mitchelson-Jacob and Sundby, 2001). These eddies occur where the NAC and NCC water meet, often during periods with prevailing north-easterly winds, and the largest eddies are often encountered to the west of Røst. It should also be noted that most of the eddies observed in Vestfjorden are of the cold core anti-cyclonic type. Since the NAC and NCC bring in Case 1 water and Case 2 water, respectively, to Vestfjorden, it may be expected that the optical signature at a given site will vary with time as a result of physical entrainment forces being stimulated on the rim of the eddies.

a TSM and Chl-*a* Concentrations

The observed variability in the concentrations of Chl-*a* and TSM for the samples collected in different seasons is shown in Table 2. The Chl-*a* concentrations were found to vary significantly with season. A maximum value of 1.94 μgL^{-1} was observed in July and a much lower minimum value of 0.17 μgL^{-1} was observed in March. The mean value of the Chl-*a* concentration shows a clear increase from 0.59 μgL^{-1} in the spring to 1.36 μgL^{-1} in the summer, and then a decrease to 0.71 μgL^{-1} in the autumn. The average Chl-*a* concentration for the whole study period was 0.75 μgL^{-1}. In April, spring-bloom Chl-*a* concentrations in Vestfjorden may reach 14 μgL^{-1} (Eilertsen and Holm-Hansen, 2000). Our low values indicate that they represent non-bloom conditions.

The observed mean value for the TSM concentration was found to be highest in the spring (1.53 mgL^{-1}), lowest in the summer (0.66 mgL^{-1}), and in between these values in the autumn (1.08 mgL^{-1}), as shown in Table 2. Averaged over all samples, the

Table 2
TSM and Chl-*a* concentrations measured in the sea around Røst in different seasons during the years 2012–2015. 'Max', 'Min', and 'STD' stand for maximum, minimum and standard deviation, respectively, and 'N' is the number of samples.

Season	TSM [mgL^{-1}]					Chl-*a* [μgL^{-1}]				
	Max.	Min.	Mean	STD	N	Max.	Min.	Mean	STD	N
Spring (Mar./Apr./May)	2.69	0.99	1.53	0.50	17	1.49	0.17	0.59	0.38	31
Summer (July/Aug.)	0.88	0.30	0.66	0.18	10	1.94	0.82	1.36	0.32	10
Autumn (Oct.)	1.48	0.83	1.08	0.16	25	1.93	0.18	0.71	0.47	27
Overall	2.69	0.30	1.15	0.44	52	1.94	0.17	0.75	0.48	68

concentration of TSM was found to be 1.15 mgL^{-1}. These levels agree with data for the northern North Sea in June (Eisma and Kalf, 1987), according to which the organic part of the suspended matter varied between 21 and 99%.

b CDOM Absorption

Generally, the absorption by CDOM was found to decrease approximately exponentially with increasing wavelength, and no significant differences in the absorption spectra were found throughout the study period. The frequency distributions for the CDOM absorption coefficient at 320 [$a_g(320)$] and 440 nm [$a_g(440)$] and for the spectral slope derived for the wavelength ranges 280–500 [$S_{280-500}$] and 350–500 nm [$S_{350-500}$] are shown in Fig. 2. The absorption coefficient at a reference wavelength is commonly used as a proxy for the CDOM concentration. In this study, CDOM absorption coefficients at two different reference wavelengths are given, one in the UV spectral region and the other in the visible spectral region. As shown in Table 3, $a_g(320)$ varied between 0.48 and 1.35 m^{-1} with overall mean value and standard deviation (STD) given by (0.73 ± 0.16) m^{-1}, and $a_g(440)$ varied between 0.055 and 0.32 m^{-1} with overall mean value and STD given by (0.11 ± 0.05) m^{-1}. The values of $a_g(440)$ found for this water body is in the range observed for coastal water around Europe (Babin et al., 2003) as well as for both coastal and oceanic water of the western Arctic Ocean (Matsuoka et al., 2011).

Several authors have pointed out that the absorption spectral slope S of CDOM depends both on the wavelength interval used for fitting (Twardowski et al., 2004; Nelson and Siegel, 2013) and on the fitting methods (Stedmon et al., 2000; Matsuoka et al., 2011), making it difficult to compare spectral slope values reported in the literature. For instance, the spectral slopes could be derived using a linear method according to which a natural logarithm transformation is performed to measured absorption spectra and then they are fitted to the natural logarithm transformation of Eq. (2). Alternatively, a nonlinear method, according to which the measured absorption spectrum is directly fitted to Eq. (2) could be used. Spectral slope values derived using a nonlinear method tend to be slightly higher than those derived by using a linear method (Stedmon et al., 2000; Twardowski et al., 2004; Matsuoka et al., 2011). The wavelength-range dependence is demonstrated in Fig. 3 (a), which shows a scatter plot of $S_{280-500}$ vs. $S_{350-500}$ for the CDOM samples collected in our study. According to our data, on average $S_{280-500}$ is 43% higher than $S_{350-500}$, demonstrating how strongly the spectral slope depends on the wavelength interval used for fitting. Therefore, it is important to specify the spectral range for which S is calculated, and care should be taken comparing S values in the literature derived for different wavelength ranges. Based on our data, a linear relationship between $S_{350-500}$ and $S_{280-500}$ can be described by $S_{280-500} = 0.848 \times S_{350-500} + 0.0089$ ($R^2 = 0.64, N = 109$).

According to Green and Blough (1994), high S values (> 0.030 nm^{-1}) and low S values (< 0.014 nm^{-1}) indicate water of

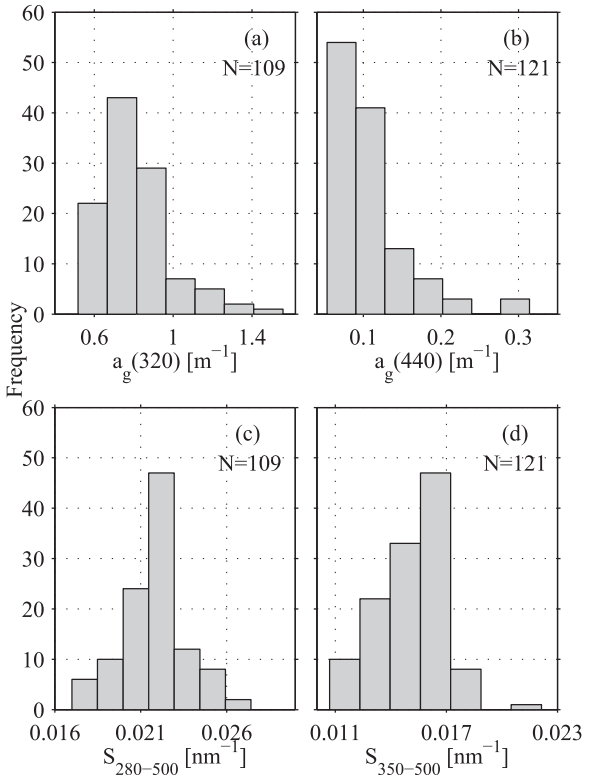

Fig. 2. Frequency distribution for the CDOM absorption coefficient at (a) 320 nm and (b) 440 nm for coastal water around Røst for different seasons during the years 2012–2015. The CDOM absorption spectral slope (c) $S_{280-500}$ and (d) $S_{350-500}$ for coastal water around Røst for different seasons during the years 2012–2015.

oceanic and terrestrial origin, respectively. $S_{280-500}$ for Røst water was found to vary between 0.017 and 0.027 nm^{-1} with overall mean value and STD given by (0.022 ± 0.002) nm^{-1}. Regardless of the wavelength range and method used for fitting, the derived mean value for $S_{280-500}$ for Røst water is slightly lower than that derived for Kattegat-Skagerrak water South of Norway, where the mean value for $S_{250-450}$ was found to be 0.023 nm^{-1} (Højerslev and Aas, 2001), but higher than that derived for Samnangerfjord, western Norway ($S_{275-425}$ = 0.017 nm^{-1} (Frette et al., 2004)), NCC water off south-western Norway ($S_{275-425}$ = 0.018 nm^{-1} (Erga et al., 2005)), and Lysefjord, western Norway ($S_{300-400}$ = 0.016 nm^{-1} (Erga et al., 2012)). Note, however, that Erga et al. (2005) found $S_{275-425}$ to vary between 0.011 and 0.032 nm^{-1} across the NCC.

The derived values for $S_{350-500}$ vary between 0.011 nm^{-1} and 0.022 nm^{-1} with overall mean value and STD given by (0.015 ± 0.002) nm^{-1}. By applying the same method as that of Babin et al. (2003), we found the mean value for $S_{350-500}$ to be 0.015 nm^{-1}, which is close to the mean value derived for coastal water for the North Sea (0.0167 nm^{-1}), but smaller than the mean

Table 3
CDOM absorption coefficients at 320 nm [$a_g(320)$] and 440 nm [$a_g(440)$], CDOM absorption spectral slopes $S_{280-500}$ and $S_{350-500}$, TSM absorption coefficient at 440 nm [$a_p(440)$], and phytoplankton absorption coefficient at 440 nm [$a_{ph}(440)$] for coastal water around Røst in different seasons during the years 2012–2015. 'Max.', 'Min.', and 'STD' stand for maximum, minimum, and standard deviation, respectively, and 'N' is the number of samples. The mark 'x' means that data were not available.

Quantity	Season	Max.	Min.	Mean	STD	N
$a_g(320)$ [m^{-1}]	Spring	1.35	0.48	0.73	0.20	63
	Summer.	x	x	x	x	x
	Autumn	0.94	0.62	0.73	0.08	46
	Overall	1.35	0.48	0.73	0.16	109
$a_g(440)$ [m^{-1}]	Spring	0.32	0.062	0.12	0.06	63
	Summer	0.20	0.081	0.13	0.04	12
	Autumn	0.15	0.055	0.095	0.02	46
	Overall	0.32	0.055	0.11	0.05	121
$S_{280-500}$ [nm^{-1}]	Spring	0.026	0.017	0.021	0.002	63
	Summer	x	x	x	x	x
	Autumn	0.027	0.019	0.023	0.002	46
	Overall	0.027	0.017	0.022	0.002	109
$S_{350-500}$ [nm^{-1}]	Spring	0.018	0.011	0.015	0.002	63
	Summer	0.016	0.012	0.013	0.001	12
	Autumn	0.022	0.014	0.016	0.001	46
	Overall	0.022	0.011	0.015	0.002	121
$a_p(440)$ [m^{-1}]	Spring	0.051	0.013	0.028	0.012	29
	Summer	0.11	0.068	0.098	0.014	8
	Autumn	0.084	0.025	0.043	0.015	27
	Overall	0.11	0.013	0.043	0.026	64
$a_{ph}(440)$ [m^{-1}]	Spring	0.041	0.007	0.021	0.011	29
	Summer	0.095	0.052	0.082	0.014	8
	Autumn	0.075	0.021	0.032	0.013	27
	Overall	0.095	0.007	0.034	0.023	64

value for coastal water of the Atlantic Ocean (0.0172 nm^{-1}) and the English Channel (0.0174 nm^{-1}) (Babin et al., 2003).

Fig. 3 (b) shows that there is an inverse linear relationship between $S_{350-500}$ and the base 10 logarithm of $a_g(440)$ for this water body (R^2=0.79,N=121), similar to that found for western Arctic water (Matsuoka et al., 2011). High S values have been associated with aging sea water in which photomineralization of dissolved organic matter (DOM) typically takes place (Obernosterer and Benner, 2004). No pronounced relationship was found between $S_{280-500}$ and $a_g(320)$. We applied the same equation used for coastal and oceanic water of the western Arctic Ocean (Matsuoka et al., 2011) to derive parameters for the coastal water around Røst. The slope derived for the Røst water (0.0115) is smaller than that found for coastal and oceanic water of the western Arctic Ocean (0.0136) (Matsuoka et al., 2011), but the intercept is higher (0.0037 vs. 0.0014). The variation of $a_g(440)$ and $S_{350-500}$ with season found for Røst water is different from that of the western Arctic ocean. For Røst water, the mean value for $a_g(440)$ was found to be almost the same in spring and summer, but to decrease from summer to autumn, while $S_{350-500}$ was found to be slightly decreasing from spring to summer and then increasing from summer to autumn. In contrast, Matsuoka et al. (2011) found the values for $a_g(440)$ in autumn to be higher than in spring and summer, and the value for $S_{350-500}$ to increase from spring to summer and then decrease from summer to autumn. They attributed such variations to accumulative injections of coastal waters into the Arctic as well as newly formed CDOM *in situ*. According to Helms et al. (2008), light exposure may lead to a decrease in CDOM molecular weight (MW) due to photobleaching of chromophores having high MW CDOM. Therefore, long-lasting light exposure of CDOM may lead to a shift from a dominance of high-MW compounds to low-MW compounds that absorb at shorter wavelengths, and thus to an inverse relationship between log a_g (440) and $S_{350-500}$ (Fig. 3b).

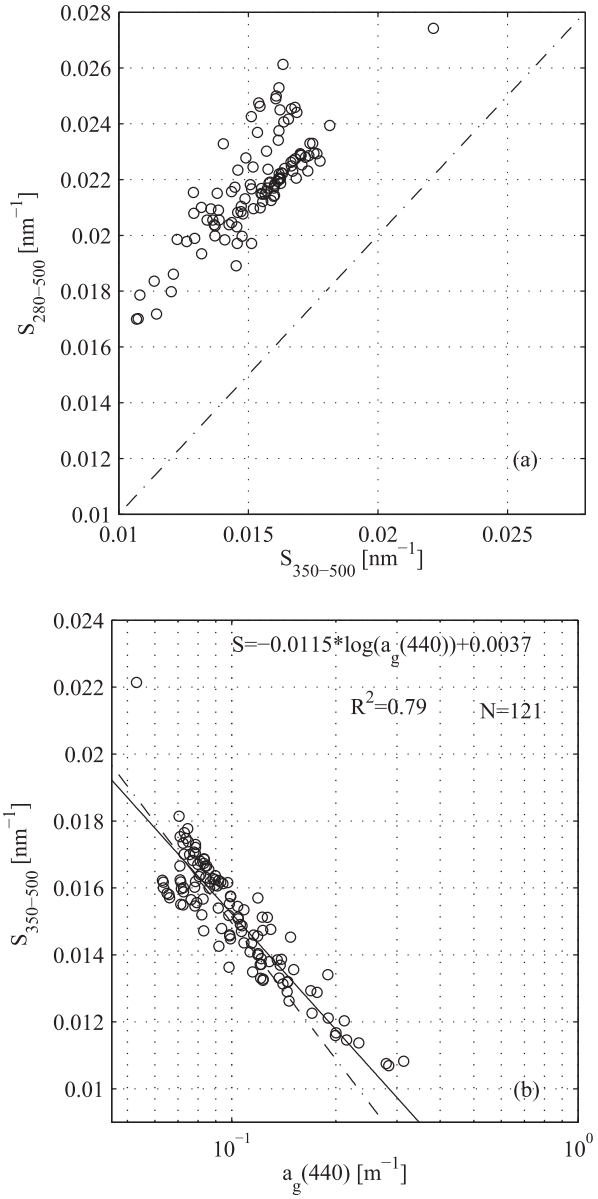

Fig. 3. (a) Scatter plot of $S_{350-500}$ against $S_{280-500}$ for the CDOM samples from the coastal water around Røst, where the dash-dotted line is the 1:1 line. (b) Relationship between the absorption spectral slope $S_{350-500}$ for CDOM and the absorption coefficient at 440 nm [$a_g(440)$]. The solid line is the fitted line using the equation shown in the figure and the dash-dotted line is the fitted line using the equation S = −0.0136 log($a_g(440)$) + 0.0014 derived for the western Arctic Ocean (Matsuoka et al., 2011). The coefficient of determination R^2 and the number N of samples are shown.

c Particle Absorption

The spectral absorption coefficients for TSM [$a_p(\lambda)$], phytoplankton [$a_{ph}(\lambda)$], and non-algal particles [$a_{NAP}(\lambda)$] for all samples are shown in Fig. 4.

TSM

Even though the observed TSM concentrations were lower in July/August than in April and October (see Table 2), the measured TSM absorption is generally higher in July/August than in March/April/May and October, as shown in Fig. 4 (a). The high absorption by TSM found in July/August is in agreement with the high

concentrations of Chl-*a* observed for the samples collected in July/August, implying that the measured TSM absorption is more closely related to the Chl-*a* concentration than to the TSM concentration. The absorption coefficients for TSM at 440 nm [$a_p(440)$] shown in Table 3 for all samples varied between 0.013 m^{-1} in March and 0.11 m^{-1} in July.

The total absorption in a water column is the sum of the absorption by water itself, CDOM, and TSM. Disregarding the absorption due to water itself, we found the total non-water absorption to be dominated by the CDOM absorption at wavelengths shorter than 600 nm, regardless of season. For instance, at 440 nm, where the phytoplankton absorption is maximal, the TSM absorption [$a_p(440)$] is much lower than the CDOM absorption [$a_g(440)$] for all seasons (see Table 3). The observed high contribution of CDOM to the total non-water absorption is consistent with previous findings for high-latitude water (Matsuoka et al., 2011), but is ten times higher than that given for north atlantic water (Kirk, 1994).

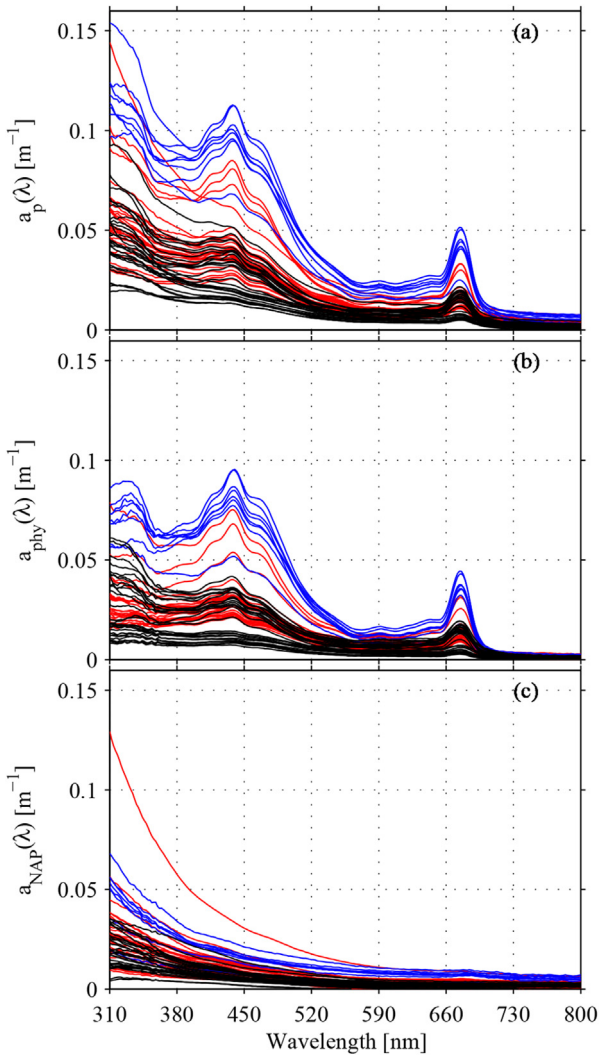

Fig. 4. Absorption coefficient due to (a) TSM [$a_p(\lambda)$], (b) phytoplankton [$a_{ph}(\lambda)$], and (c) non-algal particles [$a_{NAP}(\lambda)$] for coastal water around Røst. The black curves represent spring (March/April/May), the blue curves represent summer (July/August), and the red curves represent autumn (October). (For interpretation of the references to color in this figure legend, the reader is referred to the web version of this article.)

Phytoplankton

Distinctive peaks around 440 and 676 nm due to Chl-*a* absorption were found for the phytoplankton samples collected in July/August coinciding with the Chl-*a* concentration, while the corresponding peaks were found to be less distinctive for the samples collected in March/April/May and for most of samples collected in October, as shown in Fig. 4 (b). For all samples, the absorption coefficient for phytoplankton at 440 nm [$a_{ph}(440)$] varied between 0.007 m^{-1} observed in March and 0.095 m^{-1} observed in July (see Table 3). Phytoplankton were responsible for the dominant contribution to the TSM absorption coefficient [a_p]. The average of the ratio of the absorption coefficient for phytoplankton to that for TSM (a_{ph}/a_p) at 443, 490, and 555 nm was 73%, 71%, and 47%, respectively, in spring, 83%, 80%, and 62%, respectively, in summer, and 74%, 74% and 72%, respectively, in autumn. These wavelengths correspond to channels of the SeaWiFs instrument.

Fig. 5 shows the spectra of $a_{ph}(\lambda)$ normalized to the Chl-*a* concentration, which is called the Chl-*a* specific absorption coefficient of phytoplankton $a^*_{ph}(\lambda)$. For wavelengths shorter than 550 nm, we see that the mean value of $a^*_{ph}(\lambda)$ is slightly higher in autumn and summer than in spring. This seasonal variation of $a^*_{ph}(\lambda)$ is difficult to explain since we did not do any detailed pigment analysis, but it could be connected to variation in the dominant phytoplankton species with time. Previous observations have shown that diatoms and the prymnesiophyte *Phaeocystis pouchetii* are the main phytoplankton species in early March to early May in the Norwegian sea and Vestfjorden, while in summer the abundance of diatoms decreases to be replaced by coccolithophorids, dinoflagellates and other flagellates (Eilertsen and Holm-Hansen, 2000; Loeng and Drinkwater, 2007). This kind of change in dominant phytoplankton species with season is reflected to a certain extent in the optical properties (Stramska et al., 2003). The Chl-*a* specific absorption coefficient of phytoplankton $a^*_{ph}(\lambda)$ depends both on the package effect and the pigment composition (Bricaud et al., 2004). The higher mean value at short wavelengths for $a^*_{ph}(\lambda)$ found in summer and autumn than in spring for Røst water

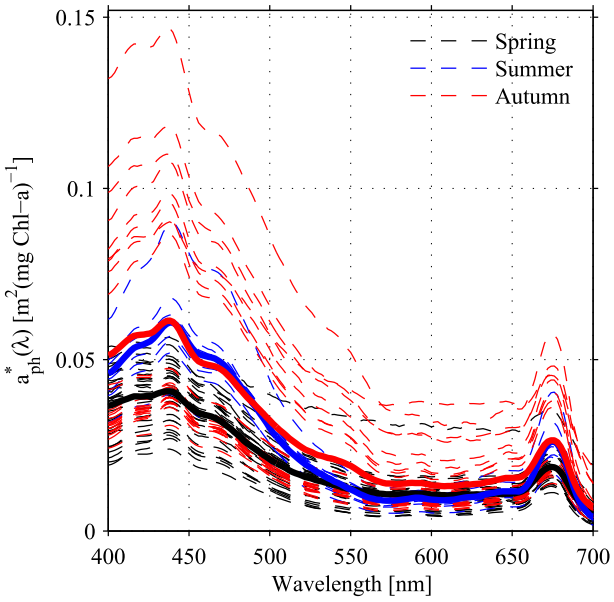

Fig. 5. Spectra of Chl-*a* specific absorption by phytoplankton obtained in spring, summer, and autumn for the Røst coastal water (dashed curves). The solid curves show the mean spectra for different seasons.

could be due to the same reason as that given by Stramska et al. (2006). They found $a^*_{ph}(\lambda)$ to be higher in summer than in spring in north polar Atlantic water at 70°–80° N latitudes, and attributed this seasonal variation, partly to the pigment package effect, but mainly to a higher proportion of total accessory pigments including photoprotective carotenoids, photosynthetic carotenoids, chlorophyll *b* and chlorophyll *c* in summer populations of phytoplankton than in spring populations. The higher $a^*_{ph}(\lambda)$ values for autumn in Fig. 5 are derived for the samples collected in October 2013. They are generally higher than those derived for the samples collected in October 2014. We believe that the difference between the $a^*_{ph}(\lambda)$ values found in October 2013 and October 2014 comes mainly from optical conditions within the cells of the phytoplankton population, which may vary in species composition from one year to another, so that both the packaging effect and different pigment types could contribute to the difference. The Chl-*a* specific absorption coefficient of phytoplankton for Røst water at 440 nm was 0.041, 0.061, and 0.061 for spring, summer, and autumn, respectively, with mean value of 0.052 m^2 mg^{-1}. The Chl-*a* specific absorption coefficient of phytoplankton for Røst water at 676 nm was 0.019, 0.026, and 0.027 for spring, summer, and autumn, respectively, with mean value of 0.023 m^2 mg^{-1}. In general, for oceanic phytoplankton corresponding to 1 μg Chl-*a* L^{-1}, specific absorption coefficients are expected to have values around 0.025 m^2 mg^{-1} at 440 nm and 0.015 m^2 mg^{-1} at 670 nm (Morel and Prieur, 1977).

According to Bricaud et al. (1998), the absorption of TSM and phytoplankton can be parameterized in terms of the Chl-*a* concentration using a power law, i.e.

$$a(\lambda) = A(\lambda) < chl >^{E(\lambda)}, \quad (6)$$

where $A(\lambda)$ and $E(\lambda)$ are wavelength dependent parameters either for TSM or phytoplankton, $\langle chl \rangle$ is the Chl-*a* concentration, and $a(\lambda)$ is either the absorption coefficient for TSM or phytoplankton. Bricaud et al. (1998) derived the spectral variation for $A(\lambda)$ and $E(\lambda)$ for oceanic water (Case 1 water) at middle and low latitudes. Regardless of season, we found the Chl-*a* absorption to be the dominant component of the TSM absorption, a situation similar to that for Case 1 water. It is of interest to see to whether this parameterization might be used also for Case 2 water, and how the wavelength dependent parameters $A(\lambda)$ and $E(\lambda)$ then would differ from those of Bricaud et al. (1998) for Case 1 water. Fig. 6 (a) shows that each of the parameters $A_p(\lambda)$ and $A_\varphi(\lambda)$ for Røst coastal water has a spectral behavior that is similar to the corresponding parameter of Bricaud et al. (1998) ($BA_p(\lambda)$ and $BA_\varphi(\lambda)$ in Fig. 6 (a)). In contrast, the parameters $E_p(\lambda)$ and $E_\varphi(\lambda)$, shown in Fig. 6 (b), have significantly different spectral behaviors than the corresponding parameters of Bricaud et al. (1998) ($BE_p(\lambda)$ and $BE_\varphi(\lambda)$). The very similar spectral variation (except in the green region) of $BE_p(\lambda)$ and $BE_\varphi(\lambda)$ probably reflects a dominance of pigmented particles in Case 1 water. In general, the average cell size and the Chl-*a* concentration tend to decrease from nutrient-rich to nutrient-poor water, where phycobilin containing picoplanktonic cyanophytes (< 2 μm) often dominate (Agawin et al., 2000). The difference between the spectra for $E_\varphi(\lambda)$ and $BE_\varphi(\lambda)$ could therefore be due to a stronger pigment package effect and a different pigment composition in Vestfjorden (where larger phytoplankton types are more common, see above) compared to what is found in the more oligotrophic types of water investigated by Bricaud et al. (1998). However, our result for $E_\varphi(\lambda)$ has a similar spectral behavior as E_φ derived for northern high-latitude water (Stramska et al., 2003) and E_φ derived at 9 wavelengths for western Norwegian fjord water (Hamre et al., 2003). The difference between E_φ for Røst water and that found by Bricaud et al. (1998) for Case 1 water could also be partly due to phaeopigment absorption, at least at short wavelengths (400–450 nm). Babin et al. (2003) found occurrence of high phaeopigment concentrations for phytoplankton in coastal water to result in deviations from the phytoplankton absorption derived by applying the Bricaud et al. (1998) statistic result (See Fig. 7 (d) and (e) in (Babin et al. 2003)). Also, deviations may be partly explained by the application of different methods for bleaching (extraction) of pigments between our study and the study by Stramska et al. (2003) compared to the study by Bricaud et al. (1998). In the former two studies, sodium-hypochloride (NaClO) was used for bleaching of pigments, whereas methanol was used in the study of Bricaud et al. (1998), which will not include the water soluble phycobilines. The A_φ and E_φ values at 676 nm, where the Chl-*a* absorption is dominant and least effected by other pigments, are 0.020 and 0.88, respectively, for Røst water. These values are quite close to those derived for oceanic water: $A_\varphi = 0.018$ and $E_\varphi = 0.82$ (Bricaud et al., 1998). It should be noted that the Bricaud et al. (1998) study also includes high productive upwelling areas and estuaries. The values of our A_p and E_p at 676 nm are 0.024 and 0.83, while the values of the corresponding parameters derived by Bricaud et al. (1998) are 0.021 and 0.82.

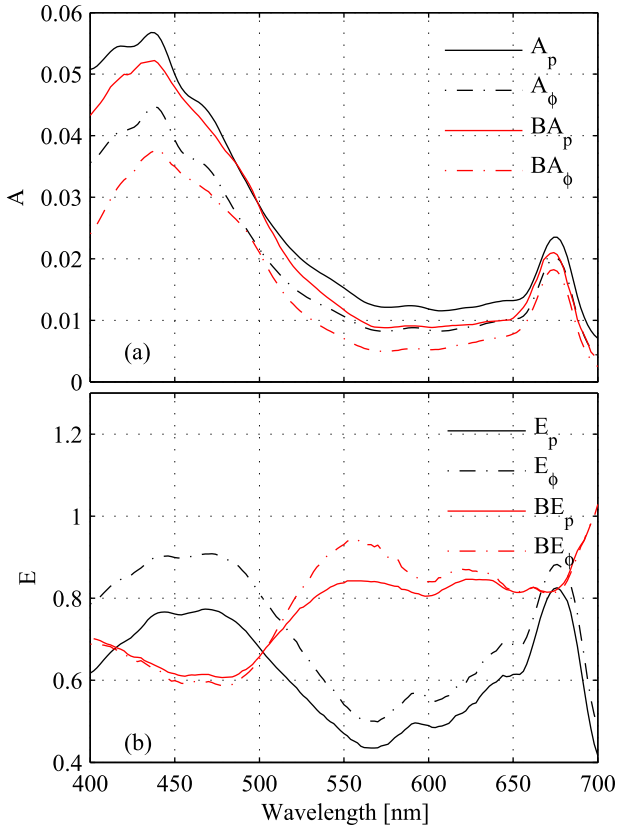

Fig. 6. Spectral parameters (a) $A(\lambda)$ and (b) $E(\lambda)$ in Eq. (6) for Røst coastal water. A_p and E_p are derived for TSM, and A_φ and E_φ are derived for phytoplankton. The spectral parameters $BA_p(\lambda)$ and $BE_p(\lambda)$ for TSM and $BA_\varphi(\lambda)$ and $BE_\varphi(\lambda)$ for phytoplankton derived by Bricaud et al. (1998) for Case 1 water are also shown.

Non-algal particles

The absorption spectra for non-algal particles are shown in Fig. 4 (c) for all samples, and are seen to increase approximately exponentially with decreasing wavelength, as is commonly found for natural water (Kirk, 1994).

Fig. 7 shows the frequency distribution of the absorption coefficient at 443 nm [$a_{NAP}(443)$] and the absorption spectral slope S_{NAP} for non-algal particles. The values of $a_{NAP}(443)$ were found to vary

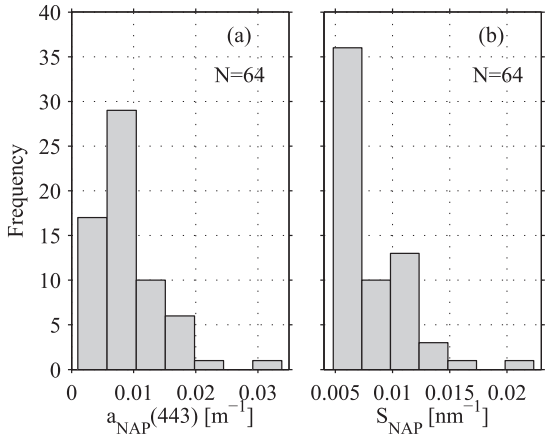

Fig. 7. Frequency distribution for (a) the non-algal particle absorption coefficient at 443 nm and (b) the non-algal particle absorption spectral slope.

between 0.001 and 0.034 m^{-1} with overall mean value and STD given by (0.0091 ± 0.006) m^{-1}. This range of values for $a_{NAP}(443)$ corresponds to the lower half of the range observed for coastal waters around Europe (Babin et al., 2003). On average, for Røst water the value of $a_{NAP}(443)$ in summer (0.017 m^{-1}) was found to be higher than those in spring (0.006 m^{-1}) and autumn (0.01 m^{-1}).

The values of S_{NAP} for Røst water were found to vary between 0.0048 and 0.022 nm^{-1} with overall mean value and STD given by (0.0083 ± 0.003) nm^{-1}. This range of values for S_{NAP} is larger than that found for coastal waters around Europe (Babin et al., 2003). For Røst water, S_{NAP} values in summer were found to be mainly distributed around 0.0053 nm^{-1} (0.0048–0.0058 nm^{-1}, Mean = 0.0053, N = 8), and in autumn they varied from 0.005 to 0.015 nm^{-1} (Mean = 0.0087, N = 27). In spring an even wider variation range of S_{NAP} values was found (0.006–0.022 nm^{-1}, Mean = 0.0087, N = 29), which may be partly attributed to the difference in time of sample collection. The mean value of S_{NAP} derived for Røst water is smaller than the corresponding mean value for coastal waters around Europe (Babin et al., 2003), but higher than the value found for the Samnanger fjord in western Norway (Hamre et al., 2003). The ratio of the absorption coefficient for non-algal particles at 443 to the TSM concentration ($a_{NAP}(443)$/[*TSM*]) was found to vary between 0.002 and 0.045 m^2 mg^{-1}. In general, it was found to be higher for the samples collected in summer (0.015–0.045 m^2 mg^{-1}) than for the samples collected in spring and autumn (0.002–0.014 m^2 mg^{-1}), which may imply that there were more organic and less inorganic particles in the summer than in spring and autumn. As a result, the TSM concentration would remain the same, while a_{NAP} (443) would increase. Such a relationship between $a_{NAP}(443)$ and TSM concentration is in agreement with Babin et al. (2003).

d Comparison of *in situ* and laboratory measured absorption coefficients

The ac-9 instrument was calibrated in pure water, so that the measured absorption in the field excluded the contribution due to pure water. Hence, the ac-9 instrument measures the absorption by particulate matter and CDOM combined. For the samples collected during the field campaign in October 2014 and in March 2015, we have both absorption coefficients measured in the field and in the laboratory. Fig. 8 shows a scatter plot of the absorption coefficient obtained from *in situ* measurements using an ac-9 instrument against that obtained by adding the absorption due to particulate matter and CDOM [a_{p+g}], which were measured separately in the laboratory, as described above. It shows that the absorption coefficient measured in the field using an ac-9 instrument and that obtained by adding the absorption due to particulate matter and CDOM measured separately in the laboratory agree quite well with high coefficient of determination R^2=0.89. The good agreement is partly attributed to a well-calibrated ac-9 instrument. For optically clean water, the absorption due to water constituents tend to be low, requiring an instrument that must be well calibrated in order to provide accurate *in situ* measurements. Also, the good agreement is a verification of the quality of the procedure used to obtain particulate matter and CDOM absorption in the laboratory.

4. Conclusions

In summary, for Røst water, the Chl-*a* concentration was found to vary with season, with highest values found in July and lowest values in October. CDOM was found to be the dominant absorber for wavelengths shorter than 600 nm regardless of season. The absorption spectral slope for CDOM was found to depend on the wavelength interval used for fitting. The absorption spectral slope $S_{350-500}$ for CDOM varied between 0.011 and 0.022 nm^{-1} with mean value and STD given by (0.015 ± 0.002) nm^{-1}, whereas $S_{280-500}$ varied between 0.017 and 0.027 nm^{-1} with mean value and STD given by (0.022 ± 0.002) nm^{-1}. Both $S_{280-500}$ and $S_{350-500}$ were found to be a little higher in October than in March/April/May. A strong linear relationship was found between the base 10 of logarithm of the absorption coefficient at 440 nm [$\log a_g(440)$] and $S_{350-500}$. For particulate matter, absorption due to TSM and phytoplankton was higher in summer with high concentration of Chl-*a* than in spring and autumn. The measured TSM absorption was found to be more closely related to the Chl-*a* concentration than to the TSM concentration. Phytoplankton was the dominant absorbing contributor to the TSM absorption regardless of season. The Chl-*a* specific absorption coefficient for phytoplankton $a^*_{ph}(\lambda)$ was found to vary with season and to be higher in autumn and in summer than in spring for wavelengths shorter than 550 nm. The absorption spectral slope S_{NAP} for non-algal particles was lower than that for European coastal

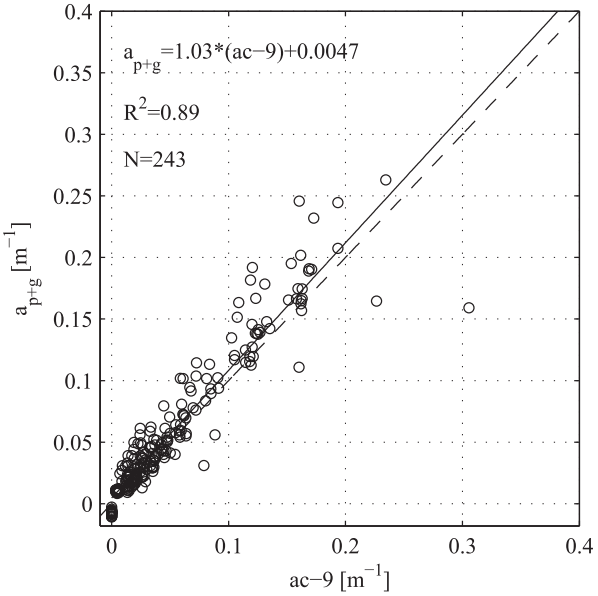

Fig. 8. Scatter plot of the absorption coefficients due absorption by particulate matter and CDOM measured in the laboratory (a_{p+g}) at wavelengths 412, 440, 488, 510, 532, 555, 650, 676, and 715 nm against the absorption coefficient obtained from *in situ* measurement with an ac-9 instrument. The solid line is the least squares fitting line, and the dashed line is the 1:1 line.

water in general. It varied between 0.0048 and 0.022 nm^{-1} with mean value and STD given by $(0.0083 \pm 0.003)\ nm^{-1}$.

Acknowledgements

This work was supported by the Network for University Cooperation Tibet-Norway (Ph.D. Fellowship to Ciren Nima and Project entitled «Environmental Physics in Tibet»), the Norwegian Research Council (Project No. 212019/F50).

References

Agawin, N.S.R., Duarte, C.M., August, S., 2000. Nutrient and temperature control of the contribution of picoplankton to phytoplankton biomass and production. Limnol. Oceanogr. 45, 591–600.
Babin, M., Stramski, D., Ferrari, G.M., Claustre, H., Bricaud, A., Obolensky, G., Hoepffner, N., 2003. Variations in the light absorption coefficients of phytoplankton, nonalgal particles, and dissolved organic matter in coastal waters around Europe. J. Geophys. Res. 108, 4.1–4.20.
Bricaud, A., Claustre, H., Ras, J., Oubelkheir, K., 2004. Natural variability of phytoplanktonic absorption in oceanic waters: influence of the size structure of algal populations. J. Geophys. Res. 109, 1–12.
Bricaud, A., Morel, A., Babin, M., Allali, K., Claustre, H., 1998. Variations of light absorption by suspended particles with chlorophyll *a* concentration in oceanic (Case 1) waters: analysis and implications for bio-optical models. J. Geophys. Res. 103, 31033–31044.
Bricaud, A., Morel, A., Prieur, L., 1981. Absorption by dissolved organic matter of the sea (yellow substance) in the UV and visible domains. Limnol. Oceanogr. 26, 43–53.
Conmy, R.N., Coble, P.G., Chen, R.F., Gardner, G.B., 2004. Optical properties of colored dissolved organic matter in the Northern Gulf of Mexico. Mar. Chem. 89, 127–144.
Dierssen, H.M., Smith, R.C., 2000. Bio-optical properties and remote sensing ocean color algorithms for Antarctic Peninsula waters. J. Geophys. Res. 105, 26301–26312.
Eilertsen, H.C., Holm-Hansen, O., 2000. Effects of high latitude UV radiation on phytoplankton and nekton modelled from field measurements by simple algorithms. Pol. Res. 19, 173–182.
Eisma, D., Kalf, J., 1987. Distribution, organic content and particle size of suspended matter in the North Sea. Neth. J. Sea Res. 21, 265–285.
Erga, S.R., Aursland, K., Frette, Ø., Hamre, B., Lotsberg, J.K., Stamnes, J.J., Aure, J., Rey, F., Stamnes, K., 2005. UV transmission in norwegian marine waters: controlling factors and possible effects on primary production and vertical distribution of phytoplankton. Mar. Ecol. Prog. Ser. 305, 79–100.
Erga, S.R., Ssebiyonga, N., Frette, Ø., Hamre, B., Aure, J., Strand, Ø., Strohmeier, T., 2012. Dynamics of phytoplankton distribution and photosynthetic capacity in a western Norwegian fjord during coastal upwelling: effects on optical properties. Estuar. Coast. Shelf Sci. 97, 91–103.
Frette, Ø., Erga, S.R., Hamre, B., Aure, J., Stamnes, J.J., 2004. Seasonal variability in inherent optical properties in a western Norwegian fjord. Sarsia 89, 276–291.
Green, S.A., Blough, N.V., 1994. Optical absorption and fluorescence properties of chromophoric dissolved organic matter in natural waters. Limnol. Oceanogr. 39, 1903–1916.
Hamre, B., Frette, Ø., Erga, S.R., Stamnes, J.J., Stamnes, K., 2003. Parameterization and analysis of the optical absorption and scattering coefficients in a western Norwegian fjord: a case II water study. Appl. Opt. 42, 883–892.
Hancke, K., Hovland, E.K., Volent, Z., Pettersen, R., Johnsen, G., Moline, M., Sakshaug, E., 2014. Optical properties of CDOM across the polar front in the barents sea: origin, distribution and significance. J. Mar. Syst. 130, 219–227.
Helms, J.R., Stubbins, A., Ritchie, J.D., Minor, E.C., Kieber, D.J., Mopper, K., 2008. Absorption spectral slopes and slope ratios as indicators of molecular weight, source, and photobleaching of chromophoric dissolved organic matter. Limnol. Oceanogr. 53, 955–969.
Højerslev, N.K., Aas, E., 2001. Spectral light absorption by yellow substance in the Kattegat-Skagerrak area. Oceanologia 43, 39–60.
Jeffrey, S.W., Humphrey, G.F., 1975. New spectrophotometric equations for determing chlorophylls a, b, c1 and c2 in higher plants, algae and natural phytoplankton. Biochem. Physiol. Pflanz. 167, 191–194.
Kirk, J.T.O., 1994. Light and Photosynthesis in Aquatic Ecosystems, second ed. Cambridge University Press.
Loeng, H., Drinkwater, K., 2007. An overview of the ecosystems of the Barents and Norwegian Seas and their response to climate variability. Deep-Sea Res. Pt. II 54, 2478–2500.
Matsuoka, A., Hill, V., Huot, Y., Babin, M., Bricaud, A., 2011. Seasonal variability in the light absorption properties of western Arctic waters: parameterization of the individual components of absorption for ocean color applications. J. Geophys. Res. 116, 1–15.
Matsuoka, A., Ortega-Retuerta, E., Bricaud, A., Arrigo, K.R., Babin, M., 2015. Characteristics of colored dissolved organic matter (CDOM) in the Western Arctic Ocean: relationships with microbial activities. Deep-Sea Res. Pt. II 118, 44–52.
Mitchell, B.G., Holm-Hansen, O., 1991. Bio-optical properties of Antarctic Peninsula waters: differentiation from temperate ocean models. Deep Sea Res. 38, 1009–1028.
Mitchelson-Jacob, G., Sundby, S., 2001. Eddies of Vestfjorden. Nor. Cont. Shelf Res. 21, 1901–1918.
Morel, A., Prieur, L., 1977. Analysis of variations in ocean color. Limnol. Oceanogr. 22, 709–722.
Nelson, N.B., Siegel, D.A., 2013. The global distribution and dynamics of chromophoric dissolved organic matter. Annu. Rev. Mar. Sci. 5, 447–476.
Obernosterer, I., Benner, R., 2004. Competition between biological and photochemical processes in the mineralization of dissolved organic carbon. Limnol. Oceanogr. 49, 117–124.
Röhrs, J., Christensen, K.H., Vikebø, F., Sundby, S., Saetra, Ø., Broström, G., 2014. Wave-induced transport and vertical mixing of pelagic eggs and larvae. Limnol. Oceanogr. 59, 1213–1227.
Sathyendranath, S., Cota, G., Stuart, V., Maass, H., Platt, T., 2001. Remote sensing of phytoplankton pigments: a comparison of empirical and theoretical approaches. Int. J. Remote Sens. 22, 249–273.
Stedmon, C.A., Markager, S., 2001. The optics of chromophoric dissolved organic matter (CDOM) in the Greenland Sea: an algorithm for differentiation between marine and terrestrially derived organic matter. Limnol. Oceanogr. 46, 2087–2093.
Stedmon, C.A., Markager, S., Kaas, H., 2000. Optical properties and signatures of chromophoric dissolved organic matter (CDOM) in Danish coastal waters. Estuar. Coast. Shelf Sci. 51, 267–278.
Stramska, M., Stramski, D., Hapter, R., Kaczmarek, S., Stoń, J., 2003. Bio-optical relationships and ocean color algorithms for the north polar region of the Atlantic. J. Geophys. Res. 108, 12–1–12–16.
Stramska, M., Stramski, D., Kaczmarek, S., Allison, D.B., Schwarz, J., 2006. Seasonal and regional differentiation of bio-optical properties within the north polar Atlantic. J. Geophys. Res. 111, 1–16.
Tassan, S., Ferrari, G.M., 2002. A sensitivity analysis of the Transmittance–Reflectance method for measuring light absorption by aquatic particles. J. Plankton Res. 24, 757–774.
Tilstone, G.H., Moore, G.F., Sørensen, K., Doerfeer, R., Røttgers, R., Ruddick, K.D., Pasterkamp, R., Jørgensen, P.V., 2002. Regional Validation of MERIS Chlorophyll Products in North Sea Coastal Waters. REVAMP Methodologies EVGI-CT-2001–00049.
Twardowski, M.S., Boss, E., Sullivan, J.M., Donaghay, P.L., 2004. Modeling the spectral shape of absorption by chromophoric dissolved organic matter. Mar. Chem. 89, 69–88.
Vodacek, A., Blough, N.V., DeGrandpre, M.D., Nelson, R.K., 1997. Seasonal variation of CDOM and DOC in the middle atlantic bight: terrestrial inputs and photooxidation. Limnol. Oceanogr. 42, 674–686.
WET-Labs, 2011. Ac Meter Protocol Document (Revision Q). WET Labs, Inc.
Wright, S.W., 1991. Improved HPLC method for the analysis of chlorophylls and carotenoids from marine phytoplankton. Mar. Ecol. Prog. Ser. 77, 183–196.